Modelling the Trojan Asteroids

Christopher Gallagher *University of Cambridge*

April 20, 2020

Trojan asteroids are v important. I'm going to make that paragraph a little longer to fill out the space in case this is forming some kind of error. i really hope this is long enough.

1 Introduction

The Jupiter trojans, commonly known as the Trojan asteroids, are two large groups of asteroids that share the planet Jupiter's orbit around the Sun in a 1:1 orbit resonance. These two groups are called the Greeks and the Trojans, named after opposing sides in the mythological Trojan war, and lead/trail Jupiter respectively in its orbit. They correspond to Jupiter's two stable Lagrange points: L_4, lying 60° ahead of the planet in its orbit, and L_5, 60° behind, with asteroids distributed in two elongated, curved regions around these Lagrangian points.

The first Jupiter trojan, 588 Achilles, was discovered in 1906 by the German astronomer Max Wolf [1], and a total of 7642 Jupiter trojans have been found as of February 2020 [2].

Research into Jupiter's trojan asteroids continues, with the particular focus on their origins reliant on an understanding of their orbit stability [3], [4]. This informs studies into their composition [5], as travel to these asteroids is considered for their potential in mineral mining [6] [7].

The purpose of this report is to use numerical simulation techniques to investigate the stability of orbits about these Lagrange points, demonstrating the asteroid oscillate about these points under small perturbations and quantifying the absolute distance of the asteroids from the Lagrange point (the wander) during their orbits. The impact of variation in planetary/solar mass on asteroid orbit stability will also be considered. *Signpost what is included in each section?*

2 Theoretical Background?

2.1 Lagrange Points

The asteroids exist at/near Lagrange points, defined in Lagrange's initial analysis of the three-body problem in 1772 [8], were he demonstrated the existence of five equilibrium points for an object of negligible mass orbiting under the gravitational effect of two larger masses. Three of these equilibrium points, L_1-L_3 lie on the line joining the two masses, while each of the remaining two points, L_4 and L_5, lie at the apex of an equilateral triangle with base equal to the separation of the two masses (see Figure 1). Despite all these points being potential maxima, stable motion is possible around L_4 and L_5 due to the Coriolis force [9].

While orbits between Lagrange points are also possible, this report will focus on the tadpole orbits observed as asteroids deviate from L4 and L5 [11]. *More detail?*

2.2 Theoretical Model

The three body problem, where the dynamics of three interacting bodies are determined given their initial positions and velocities, has no analytical (closed-form) solution in the general case [12].

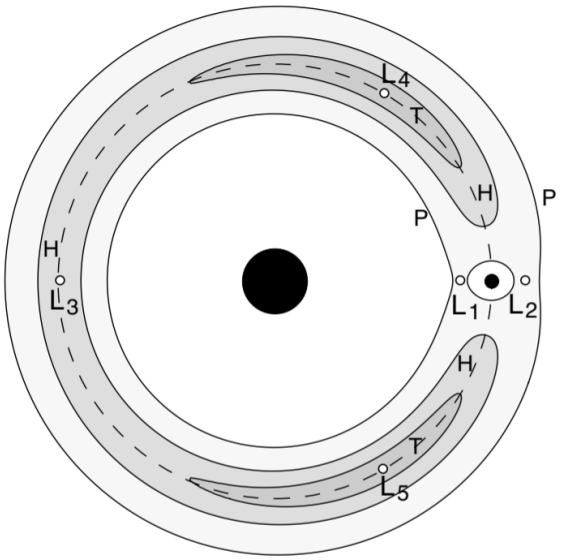

Figure 1: *The location of the five Lagrange equilibrium points in the circular-restricted three-body problem. The solar and planetary masses are denoted by the large and small filled circles, and the letters P, H, and T denote passing, horseshoe, and tadpole orbits respectively. Note that the two masses form an equilateral triangle with each of the L_4 and L_5 points. Reproduced from Marzari et al. [10]*

In this report, I will consider the circular, restricted, three-body problem, where two of the bodies move in circular, coplanar orbits about their common centre of mass, unaffected by the negligible mass of the third body. I will also assume that all interactions are via Newtonian gravity.

The system of differential coordinates determine the position and velocity of the asteroids, with two equations per spatial coordinate.

$$\frac{dr_i}{dt} = v_i, \frac{dv_i}{dt} = g_i, \quad i = x, y \tag{1}$$

In this, g_i is given by:

$$\mathbf{g} = -\frac{GM_s}{|\mathbf{r} - \mathbf{r}_s|^3}(\mathbf{r} - \mathbf{r}_s) - \frac{GM_p}{|\mathbf{r} - \mathbf{r}_p|^3}(\mathbf{r} - \mathbf{r}_p) \tag{2}$$

where the subscripts *s* and *p* refer to solar and planetary properties respectively.

We may also consider a frame rotating at the same speed as the massive bodies. As there is 1:1 orbital resonance between Jupiter and the asteroids, all three bodies are stationary in this frame. This significantly increases the accuracy of numerical simulations, as the exact solution is stationary rather then requiring an infinite power series [13], [14].

When transforming into this rotating non-inertial frame, g_i gains an additional virtual force term with coupling between the spatial coordinates. This is given below as the sum of the centripetal and Coriolis forces:

$$\Delta g_i = \Omega^2 r_i - 2[\mathbf{\Omega} \times \mathbf{v}]_i \tag{3}$$

where Ω is the angular speed of the rotating frame, and $\mathbf{v}$ is the velocity of the asteroid within this frame.

2.2.1 Assumptions - FIX

- Circular orbit
- Constant Jupiter-Sun separation
- Coplanar orbits
- Negligible asteroid mass
- Newtonian gravity

I also applied the following symmetries: trojan and greek symmetry (analysis focused on greeks) rotational symmetry - arbitrary initial point direction of orbit "The combination of these symmetries allows the problem to be simplified. Such that only the Greeks, orbiting counter-clockwise, with perturbations at t = 0, need to be investigated. " (This reduces computing time not hvaing to solve for trojans as well)

2.3 Orbit Geometry

As the three bodies considered here form an equilateral triangle in the initial equilibrium state, as depicted in Figure 2, we can derive the polar coordinates of each body with respect to the centre of mass about which the bodies orbit.

Using standard trigonometric relations, it is simple to show that the values r_a and θ are given by:

$$r_a = \sqrt{a^2 + R_s R_p}, \;\; \theta = \tan^{-1}\left(\frac{a\sin(\frac{\pi}{3})}{R_p - \frac{a}{2}}\right) \tag{4}$$

Furthermore, the Lagrange point in Cartesian coordinates based about the centre of mass is easily found to be:

$$(x, y) = \left(R_p - \frac{a}{2}, \frac{\sqrt{3}a}{2}\right) \tag{5}$$

Finally, equating the gravitational and centripetal forces on the planet allows the derivation of its (and all other bodies') orbital velocity:

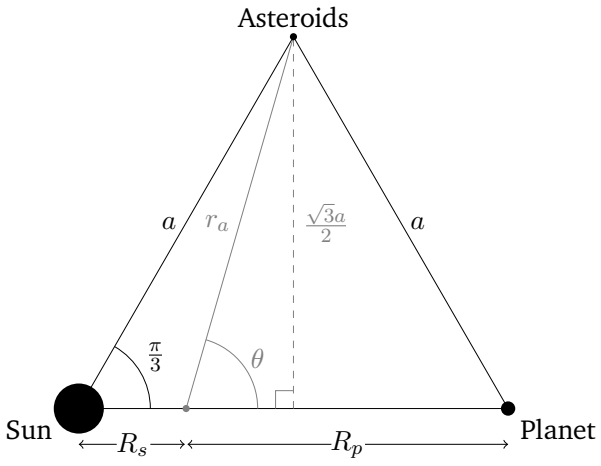

Figure 2: *A geometric depiction of the three-body system, in the case where the planet has a mass equal to a third of the sun, and asteroids are considered at the L_4 point. R_s and R_p denote the (fixed) radii from the centre of mass (the grey point) to the Sun and the planet respectively, while r_a denotes the radius of the asteroids.*

$$\Omega = \sqrt{\frac{G(M_s + M_p)}{a^3}} \tag{6}$$

3 Methodology

This system of coupled first-order ordinary differential equations (ODEs) was solved using the scipy solve_ivp function. The time span was taken as 100 orbits (with 100 points sampled per orbit) unless otherwise stated; this corresponds to 1185 Earth years. Rescaled solar system units are used for mathematical ease, so distances are measured in astronomical units (AU), time in earth years and mass in multiples of the solar mass, and to prevent floating point overflows due to the magnitude of the quantities considered in SI units.

The wander was defined as the maximum distance of the asteroid from the initial point during the orbit (for small perturbations this is also approximately the separation from the Lagrange point). Initial conditions are defined by the Lagrange point in each frame, with the initial velocity in the stationary frame defined by the period of Jupiter's orbit, and split into Cartesian components.

3.1 Integration Method

Within solve_ivp, the default solver is RK45 (an explicit Runge-Kutta method of order 5(4) [15]) however this is non-stiff, giving a deviation in asteroid position (from the Lagrange point) in the order of 10^{-4} AU in the rotating frame over 50 years. This is larger than expected, suggesting the system of equations requires an unreasonable small step size for numerically stability with respect to this numerical method, even regions where the solution curve is smooth [16]. This suggests the system is stiff, and solvers designed for this typically do more work per step, allowing them to take much larger steps, and have improved numerical stability compared to the non-stiff solvers [17].

Instead the stiff "Radau" solver (an implicit Runge-Kutta method of the Radau IIA family of order 5 [18]) is used for increased stability [19], and achieves a deviation in asteroid position in the order of 10^{-13} AU instead. This also ensures stability in the stationary frame, with deviations of 0.76% in asteroid separation from Jupiter over 10^3 years, compared to 53% for the best non-stiff solvers.

3.2 Programme Structure

Global constants such as solar mass, and sun–planet separation, along with derived values from these such as orbital period and solar radius from centre of mass, are given in an importable python module "*constants*".

Functions to evaluate these coupled differential equation systems are defined in module "*orbits*", while additional functions to evaluate the wander during the orbit (under different sampling routines) are implemented in "*wander*". Further files then import these modules and produce the plots given in this report, fully detailed in appendix A.

To consider a varying planet mass, it was considered preferable to avoid reconstructing all functions to take this as an argument as this requires re-evaluating all initial derived constants. Therefore, I iterate over alternative masses, re-defining constant values in this instance, and then directly import the required functions to compute the orbit. **REPHRASE?**

Complete code listings are given in appendix B.

3.3 Performance

Sampling 100 points per orbit for 100 orbits takes a mean time of 16.97 ± 34 ms, with sub-linear scaling for sampling rate and orbit number up to the array memory limit, achieved through the optimised integration routines within solve_ivp.

4 Results

4.1 Stability of Lagrange Points

Considering the Greeks' orbit without perturbations applied, it has a maximum deviation of 4.68×10^{-13} AU over 100 orbits (1185 years). This value is unchanged if 1000 orbits are considered instead, confirming the stability of this Lagrange point.

In the stationary frame, this wander from the (now moving) Lagrange point is depicted in Figure 3. The deviation oscillates with a magnitude of 9.10×10^{-2} AU, and a period of 148.2 ± 0.8 years, where the error was determined by the width of the Fourier peak. This is modulated with a faster oscillation component of 11.85 ± 0.27 years, equivalent to the orbital period of the asteroids and clearly demonstrating an periodic error in the integration routine, becoming more significant over time.

These much more significant errors are due to time dependence in the exact solution, as detailed in Section 2.2. Energy can also be evaluated, and conserved, in this inertial frame; asteroid specific energy varies within only 0.113% of the initial value, and with a similar periodicity to wander.

Animations show orbit....

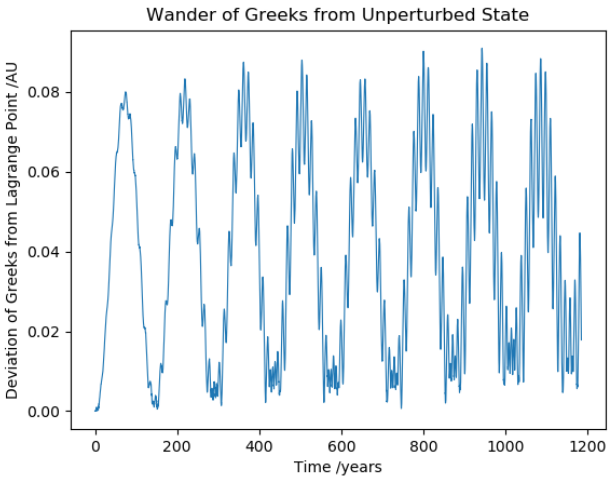

Figure 3: *The wander of Greek asteroids from the Lagrange point in the stationary frame. Note the two oscillation components and constant maximum oscillation amplitude over time, demonstrating this point is indeed stable.*

4.2 Wander Analysis

4.2.1 Perturbations in z-direction

5 Discussion

6 Conclusion

References

[1] S. B. Nicholson, "The trojan asteroids", Leaflet of the Astronomical Society of the Pacific **8**, 239 (1961).

[2] Minor Planet Centre, International Astronomical Union, *Trojan minor planets*, (2020) `https://minorplanetcenter.net//iau/lists/Trojans.html`.

[3] R. P. D. Sisto, X. S. Ramos, and T. Gallardo, "The dynamical evolution of escaped jupiter trojan asteroids, link to other minor body populations", Icarus **319**, 828–839 (2019).

[4] D. Nesvorný, D. Vokrouhlický, W. F. Bottke, and H. F. Levison, "Evidence for very early migration of the solar system planets from the patroclus–menoetius binary jupiter trojan", Nature Astronomy **2**, 878–882 (2018).

[5] M. E. Brown, "The 3–4 micrometer spectra of jupiter trojan asteroids", The Astronomical Journal **152**, 159 (2016).

[6] T. Okada, T. Iwata, J. Matsumoto, J.-P. Bibring, S. Ulamec, R. Jaumann, R. Nakamura, H. Yano, Y. Kebukawa, J. Aoki, Y. Kawai, K. Terada, M. Toyoda, M. Ito, K. Yabuta, H. Yurimoto, Y. Saito, S. Yokota, C. Okamoto, S. Matsuura, K. Tsumura, D. Yonetoku, T. Mihara, A. Matsuoka, R. Nomura, T. Hirai, N. Grand, H. Cottin, L. Thirkell, C. Briois, T. Saiki, H. Kato, O. Mori, and J. Kawaguchi, "Science and exploration of a jupiter trojan asteroid in the solar-power sail mission", in 48th lunar and planetary science conference (Mar. 2017).

[7] H. F. Levison and Lucy Science Team, "Lucy: Surveying the Diversity of the Trojan Asteroids, the Fossils of Planet Formation", in Lunar and plan-

etary science conference, Lunar and Planetary Science Conference (Mar. 2016), p. 2061.

[8]J.-L. Lagrange, "Essai sur le probléme des trois corps", Prix de l'Académie Royale des Sciences de Paris **IX** (1772).

[9]J. Lissauer and C. Murray, "Solar system dynamics: regular and chaotic motion", in *Encyclopedia of the solar system (third edition)* (2014).

[10]F. Marzari, H. Scholl, C. Murray, and C. Lagerkvist, "Origin and evolution of trojan asteroids", Asteroids III (2002).

[11]C. D. Murray and S. F. Dermott, *Solar system dynamics* (Cambridge University Press, 1999), pp. 95–102.

[12]J. Barrow Green, "The princeton companion to mathematics", in *The three-body problem*, edited by T. Gowers (Princetown University Press, 2008) Chap. V, pp. 726–728.

[13]N. Guglielmi and E. Hairer, "Implementing radau IIA methods for stiff delay differential equations", Computing **67**, 1–12 (2001).

[14]R. LeVeque, *Finite difference methods for ordinary and partial differential equations : steady-state and time-dependent problems* (Society for Industrial and Applied Mathematics, Philadelphia, PA, 2007), pp. 131–153.

[15]J. Dormand and P. Prince, "A family of embedded runge-kutta formulae", Journal of Computational and Applied Mathematics **6**, 19–26 (1980).

[16]J. D. Lambert, *Numerical methods for ordinary differential systems : the initial value problem* (Wiley, Chichester New York, 1991), pp. 217–220.

[17]G. D. Byrne and A. C. Hindmarsh, "Stiff ODE solvers: a review of current and coming attractions", Journal of Computational Physics **70**, 1–62 (1987).

[18]E. Hairer, *Solving ordinary differential equations II* (Springer, Berlin, 2010).

[19]R. Frank, J. Schneid, and C. W. Ueberhuber, "Stability properties of implicit runge–kutta methods", SIAM Journal on Numerical Analysis **22**, 497–514 (1985).

Appendix A Program Structure

Global constants, along with derived values from these are given in an importable python module "*constants*".

Functions to evaluate these coupled differential equation systems are defined in module "*orbits*", while additional functions to evaluate the wander during the orbit are implemented in "*wander*".

Wander from unperturbed initial conditions is calculated within *lagrange_stability*, with ODE solver performance also evaluated here.

Appendix B Code Listings

```
import math
import numpy as np
from scipy import integrate
import matplotlib.pyplot as plt

from constants import G, M_S, M_P, R, ORBIT_NUM, PRECISION
# User defined constants
from constants import (
    solar_rad,
    planet_rad,
    period,
    omega,
    time_span,
)  # Derived constants
```